Laser Welding of a Stent

C J Budd, Ian Hewitt, Sarah Mitchell, Chris Coles, James Rankin, David Rodrigues, Mick O'Brien, Sean McKee, Michael Vynnycky, John King, Sean McGinty

Abstract

We consider the problem of modelling the manufacture of a cylindrical Stent, in which layers of a plastic material are welded together by a Laser beam. We firstly set up the equations for this system and solve them by using a Finite Element method. We then look at various scalings which allow the equations to be simplified. The resulting equations are then solved analytically to obtain approximate solutions to the radial temperature profile and the averaged axial temperature profile.

Contents

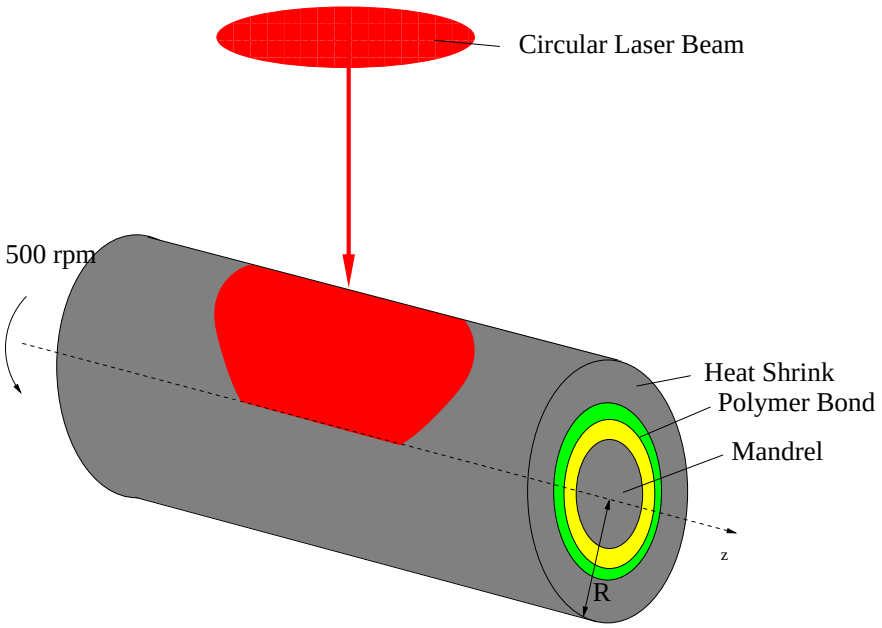

Figure 1: Typical arrangement.

1 Introduction

Stents are widely used in surgery as a means of reinforcing a damaged blood vessel. They typically comprise short cylindrical combinations of several plastic materials, a few centimetres in length and about 670μ in radius. As part of the manufacturing process these materials have to be welded together. The problem of doing this welding efficiently using a laser was brought to ESGI62 by Boston Scientific.

Laser welding works by drawing a cylindrical covering of a shrink plastic material over another smaller cyliner of Pebax. and subjecting this combination to an incident laser light. At the centre of the assembly is a mandrel which acts both as a support for the plastic materials and a significant heat sink. The laser provides localised heating on the surface which is then conducted through the material causing a weld at the interface between the shrink plastic and the Pebax, when a thin layer of the Pebax melts. To obtain an even distribution of heat, the whole material is spun rapidly at 500rpm, and it is drawn slowly past the point of laser illumination. A typical geometry for this process is illustrated balow.
The problem posed to the Study Group was to model this process and to try to determine analytical solutions for the temperature. To consider this problem we needed to take into account three issues

1. The illumination of the laser onto the material and the resulting transfer

of thermal energy from the laser.

2. The conduction of heat through the material

3. The welding process.

Each of these posed its own issues. Problem one is a nice question in geometry. Problem two is fairly classical and had an approximate analytic solution and Problem three was solved numerically using an enthalpy method.

2 Basic modelling

2.1 The model equations

The most fundamental problem in modelling the Stent manufacture is to determine how the heat generated by the laser is then transferred through the materials, and how this leads to welding. To do this we consider the whole system to be a cylinder with axial variable z with a circular cross-section with radial variable r comprising an outer layer of the Shrink, a middle layer of Pebax and an inner Mandrel. These three layers will be denoted by the index $i = 1, 2, 3$ respectively, with associated material properties. We let the temperature be $T(r, z, t)$ and the related enthalpy $e(r, z, t)$ (necessary for calculating the changes of phase during welding). Heat is generated by the laser energy which arises from the laser light striking the cylinder from above over a localised region. This energy is the absorbed by the material heating it up. Heat energy is lost by radiation at the surface and through the heat sink effect of the Mandrel in the centre.

The basic equation for the heat transfer in each of the layers is then given by

$$\rho_i \frac{\partial e}{\partial T} T_t = k_i \nabla^2 T + Q_i(r, z) e^{-\alpha_i l(r,z)}. \tag{1}$$

Here ρ_i are the material densities and k_i the thermal conductivities. The enthalpy $e(r, z, t)$ is given by the expression

$$\frac{\partial e}{\partial T} = c_i + L_i \delta(T - T_{m,i}). \tag{2}$$

Here c_i is the specific heat capacity of the material, L_i is the Latent Heat of melting, δ is the Dirac Delta function, and $T_{m,i}$ the material melting temperature. In practice, only the Pebax layer melts, in a region close to the interface with the Shrink layer. For all numerical calculations (for which we use an enthalpy method) the delta function is replaced by a regularised function.

The most subtle part of the expression in (1) are the source terms

$$Q_i(r, z) e^{-\alpha_i l(r,z)}, \tag{3}$$

in which Q_i is the surface intensity of the laser, $l(r,z)$ is the distance into the material that the laser beam has to penetrate, and α_i is the absorbtion coefficient. The exponential decay is a consequence of the well established *Lambert law* for the absorbtion of electromagnetic energy when the wave-length of the incident electromagnetic field is much smaller than the material cross-section.

A significant source of heat loss occurs at the boundary of the assembly and is due to a combination of convective and radiative effects. This leads to the boundary condition

$$-k_1 T_r = h\,(T - T_a) + \sigma T^4. \tag{4}$$

Here h is the coefficient for convective heat transfer, T_a the ambient temperature and σ the Stefan-Boltzman coefficient. Note that in this expression T corresponds to the absolute temperature. There was some discussion in the Study Group of the magnitude of the convective heat transfer term h. A value was given in the briefing document for the transfer from a material in a stationary air-flow. However, this was felt to be rather to low given that the whole assembly is rotating rapidly. This will lead to a significantly larger transfer of heat and needs to be investigated further. In experiments a maximum recorded value of $T = 480K$ was given. This implies that, given the tabulated values of h at this maximum temperature the convective and radiative heat losses are comparable. For lower values the convective heat loss dominates.

2.2 Numerical solution

The equations (1,2,3,4) can be solved directly numerically. To do this we use a Finite Element method and the resulting contours of the temperature, together with the temperature profile in the axial and radial directions at time $t = 80s$ are shown in Figure 2. Note the effect of the heat sink in the Mandrel and the localised nature of the heating of the Laser.

2.3 Some scalings and time-scales

To make analytic progress in finding the temperature profile some approximations/simplifications are necessary taking into account the different magnitude of the various terms. Some experimental values of these are given below.

Radial distance	R	670 micron
Axial distance	Z	10 mm
Rotation time	t_r	0.1s
Average density	ρ	1000kg m^{-3}
Average heat capacity	c	2200
Shrink/Pebax conductivity	k	0.3
Latent Heat of Pebax	L	37500
Melting temperature	T_m	170°C

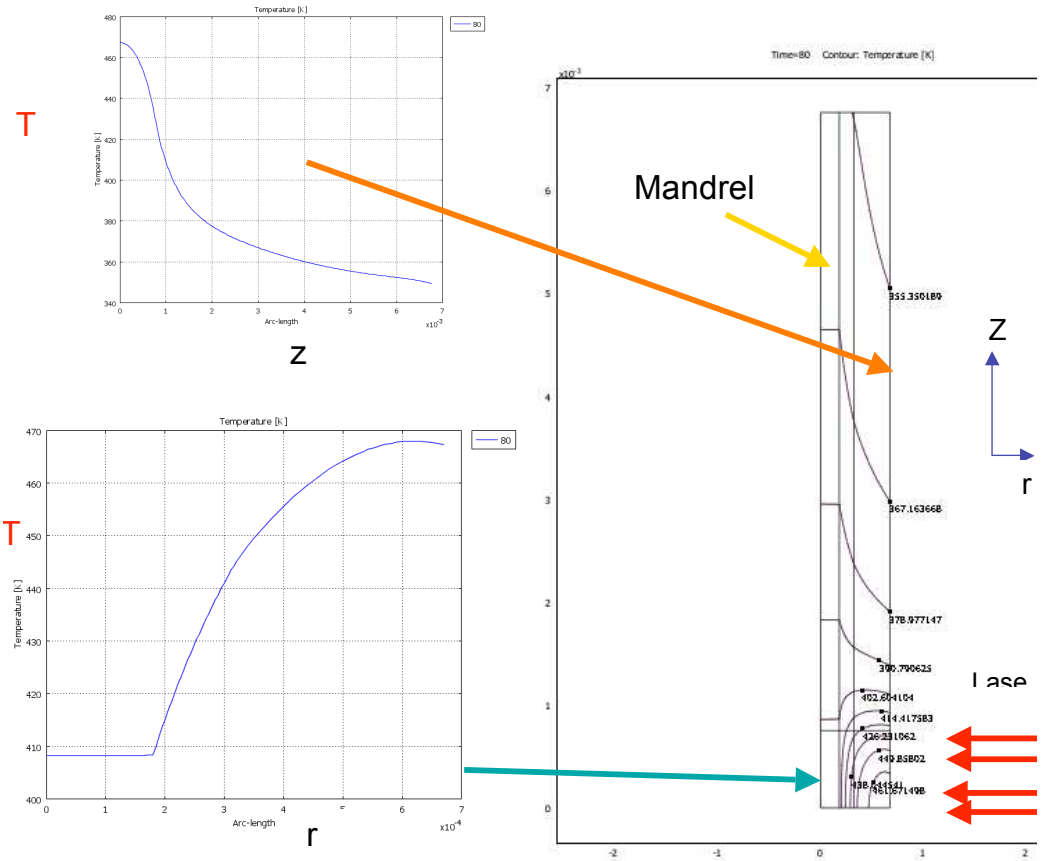

Figure 2: A numerical approximation to the solution obtained by using the Finite Element method at the time $t = 80s$. In this calculation the contours of the temperature are given on the rightmost figure in which the radial direction is horizontal and the axial direction is vertical. The system is heated by the Laser at the bottom right corner. The other two figures show the axial surface temperature (top) and the radial temperature through a cross-section (bottom)

The diffusion time-scale in the *radial* direction is then given by

$$t_d = R^2 \rho c/k \approx 1s \gg t_r.$$

We see that t_r is much greater than the rotation time. This allows us to make the great simplification that the effects of the rotation means we can average the temperature calculation over rotations.

The diffusion time-scale in the *axial* direction is given by

$$t_a = Z^2 \rho c/k \approx 60s \gg t_r.$$

It follows that the heat diffuses much more rapidly in the radial direction than in the axial direction. To calculate the temperature in the axial direction we can thus firstly consider the heat transfer in the radial direction and average $T(r, z, t)$ over a radius to give an averaged temperature $\bar{T}(z, t)$. We can then reduce the averaged system to a much simpler partial equation for the averaged temperature $\bar{T}(z, t)$. We do note however, that the thermal conductivity of the Mandrel is rather higher than that of the Pebax leading to a much greater heat loss there.

Finally we compute the Stefan number Se over a typical temperature change of $\Delta T \approx 150$ given by

$$Se = \frac{L}{c\Delta T} \approx 0.1.$$

We see that Se is rather less than one. As a consequence the energy loss at the change of phase of the Pebax is small when compared to the overall thermal energy, and the phase change does not greatly affect the temperature profile.

3 The geometry of the laser heating

The laser light forms a beam of circular cross section of radius b, with b rather greater then R. As a consequence, the beam from the laser strikes the top part of cylinder over a distributed surface with a non-trivial shape seen in Figure 3.

This is further affected by the rotation of the cylinder which averages the overall surface power over the whole of the rotated area to form an averages cylindrical region of width $2b$ subjected to heating. Clearly if the power of the laser beam is Q and this beam only strikes part of the top surface of the cylinder at any one time, then the effects of the rotation and the geometry will lead to a reduced value Q_{age} of Q in the equation for the radial temperature profile. The exact value for this depends on the ratio of b to R. If $b \gg R$ then $Q_{age} \approx Q/2$ and if $b \ll R$ then $Q_{age} \approx Q/(2R/b)$. A rough estimate made during the Study Group for the values of b and R given was

$$Q_{age} \approx \frac{Q}{3.5}. \tag{5}$$

However, this estimate should be improved in any further work and could be the subject of a nice investigation. We note that such calculations are *routine*

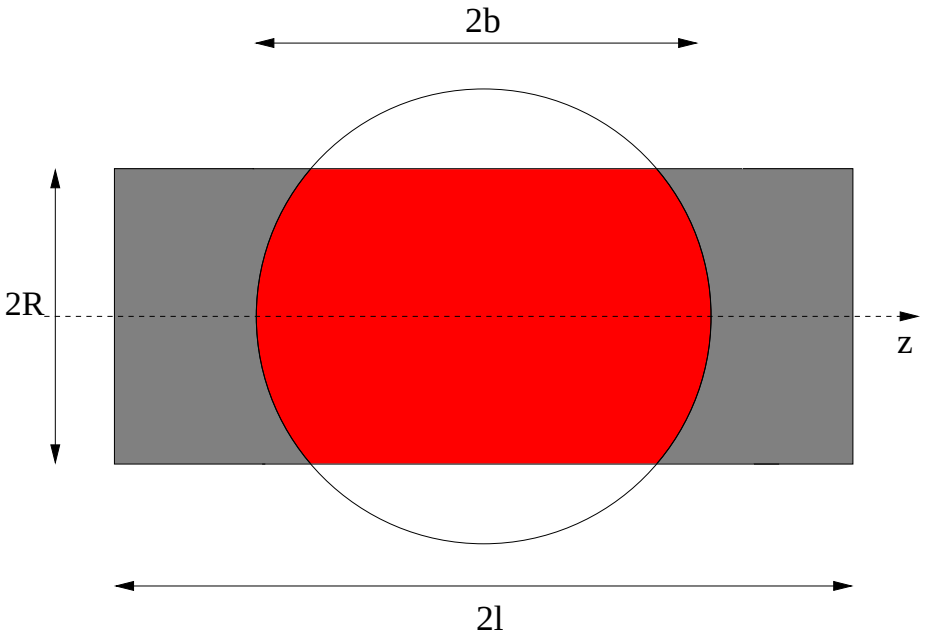

Figure 3: A plan view of the surface given by the laser light intersecting the cylinder

in the computer graphics industry in which the illumination of an object by a light source needs to be calculated. We recommend that this literature should be consulted for future studies of this system.

4 The radial temperature profile

To a first approximation, noting that the time-scale for axial heat diffusion is much less than that for radial diffusion we can solve the radial temperature profile over the heated region in the by integrating the reduced set of equations given by

$$\rho_i \frac{\partial e}{\partial T} T_t = k_i \left(T_{rr} + \frac{T_r}{r} \right) + Q_{age} e^{-\alpha_i (R-r)}, \tag{6}$$

$$\frac{\partial e}{\partial T} = c_i + L_i \delta (T - T_{m,i}), \tag{7}$$

$$-k_1 T_r = h \left(T - T_a \right) + \sigma T^4. \tag{8}$$

with the equation of continuity of heat flux across the material interfaces given by

$$k_i T_{i,r} = k_j T_{j,r}. \tag{9}$$

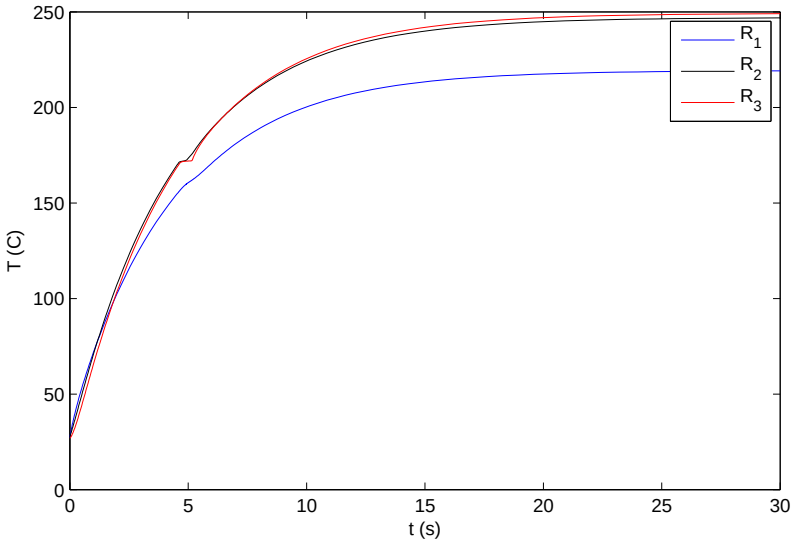

Figure 4: The change in temperature with time at radii $R_1 < R_2 < R_3$. Note the effect of the phase change leading to the welding and the associated polymer bond.

A numerical approximation to solution of this system calculated by using the Enthalpy method (with a smoothed approximation of the delta function) is given in Figure 4, for three different radii in the Mandrel (R_1), the Pebax (R_2) and the Shrink (R_3). We can see the effect of the phase change in a localised flattening in the temperature profile of the Pebax. This is a relatively small effect due to the low value of Se.

5 Averaging in the radial direction, and the axial temperature profile

Following the previous calculation, we now consider averaging the temperature over a radius. Do do this we define an *averaged temperature* $\bar{T}(z,t)$ by the expression

$$\pi R^2 \bar{T} = 2\pi \int_0^R T\, r dr \quad \text{so that} \quad \bar{T} = \frac{2}{R^2} \int_0^R T\, r dr. \tag{10}$$

Now, the rotation averaged form of (1) on the assumption that Se is small, so that the Latent heat of melting the Pebax can be ignored, takes the form

$$\rho c T_t = \frac{1}{r} \left(k r T_r \right)_r + k T_{zz} + Q_{ave} e^{\alpha(R-r)} I_{[-b,b]} \tag{11}$$

Here the indicator function $I_{[-b,b]}$ which takes the value $I = 1$ if $z \in [-b, b]$ and $I = 0$ otherwise, is used to represent the effect of the Laser beam which only strikes the surface over a limited region which we take to be the interval $z \in [-b, b]$. If we now multiply the equation (11) by r and integrate over a radius we have

$$\rho c \frac{R^2}{2} \bar{T}_t = kRT_r(R, z, t) + k\frac{R^2}{2}\bar{T}_{zz} + Q_{ave} I_{[-b,b]} \int_0^R e^{\alpha(R-r)}\, r dr.$$

Setting

$$\bar{Q} = \frac{2Q_{age}}{R^2} \int_0^R e^{\alpha(R-r)}\, r dr \tag{12}$$

we then have

$$\rho c \bar{T}_t = \frac{2k}{R} T_r + k\bar{T}_{zz} + \bar{Q} I_{[-b,b]}.$$

Now, in this expression we can substitute the boundary condition

$$-kT_r = h(T(R, z, t) - T_a) + \sigma T(R, z, t)^4$$

to give

$$\rho c \bar{T}_t = k\bar{T}_{zz} - \frac{2h}{R}(T(R, z, t) - T_a) - \frac{2\sigma}{R} T(R, z, t)^4 + \bar{Q} I_{[-b,b]}.$$

Finally, when considering the *axial* temperature distribution we observe that the time for the heat to be conducted axially is much longer than the radial conduction time. On this assumption it is a reasonable approximation to assume that the temperature is reasonably constant over a cross-section, and to replace the surface temperature by the average temperature. This gives the following partial differential equation for the averaged temperature

$$\rho c \bar{T}_t = k\bar{T}_{zz} - \frac{2h}{R}(\bar{T} - T_a) - \frac{2\sigma}{R} \bar{T}^4 + \bar{Q} I_{[-b,b]}. \tag{13}$$

It is relatively easy to find a numerical approximation to the solution to this equation by using a standard numerical method (such as the method of lines). However, to make some analytic progress we note that until $\bar{T}$ gets fairly large, the convective heat loss is rather greater than the radiative heat loss. In this case the equation simplifies to

$$\rho c \bar{T}_t = k\bar{T}_{zz} - \bar{h}(\bar{T} - T_a) + \bar{Q} I_{[-b,b]}, \tag{14}$$

where $\bar{h} = 2h/R$ (although we might want to increase the value of $\bar{h}$ in this calculation to allow for the effects of the radiative heat loss.
It is now possible to solve (14) exactly for $\bar{T}(z, t)$ by using an appropriate Green's function. To do this we will assume that the temperature is initially ambient

$\bar{T}(z,t) = T_a$, and that as $|z| \to \infty$ we have $\bar{T} \to T_a$. The resulting solution is then given by

$$\bar{T}(z,t) = T_a + q\int_0^t e^{-\lambda(t-\tau)}\left[\mathrm{erf}\left(\frac{z+b}{2\sqrt{\kappa(t-\tau)}}\right) - \mathrm{erf}\left(\frac{z-b}{2\sqrt{\kappa(t-\tau)}}\right)\right]\,d\tau. \tag{15}$$

Here $\mathrm{erf}(x)$ is the Error Function, and the various parameters in the solution are given by

$$q = \frac{\bar{Q}}{2\rho c} \approx 25, \quad \lambda = \frac{\bar{h}}{\rho c} \approx 0.1, \quad \kappa = \frac{k}{\rho c} = 1.3 \times 10^{-7}. \tag{16}$$

We note that after a time of $t = 1/\lambda \approx 10s$ the temperature approaches a limiting value. By using known results about the Error Function we can determine the asymptotic form $\bar{T}_{asy}(0,t)$ of the temperature $\bar{T}(0,t)$ at the centre of the heated section of the cylinder. This is given by

$$\bar{T}_{asy}(0,t) = \bar{T}_\infty - \frac{2qb}{\sqrt{\kappa\lambda}}\mathrm{erfc}\left(\sqrt{\lambda t}\right), \tag{17}$$

where

$$\bar{T}_\infty = T_a + \frac{2q}{\lambda}\left[\sinh\left(2\sqrt{\frac{\lambda b^2}{4\kappa}}\right) + 1 - \cosh\left(2\sqrt{\frac{\lambda b^2}{4\kappa}}\right)\right]. \tag{18}$$

To illustrate the solution, in Figure 5 we present the averaged temperature $\bar{T}(z,t)$ as a function of z for various times $t = 0s, 10s, 20s, 30s$ and in Figure 6 we present the centre temperature $\bar{T}(0,t)$, comparing the exact and the asymptotic solutions.

6 Conclusions

The formulae presented in the last section, when combined with the Finite Element calculations presented in Section 2, allow a reasonably detailed study of the temperature profile. The various scalings determined indicate that, although the heating process is a subtle nonlinear one, it is possible to approximate it with a more tractable system. However, to do this we have had to make some considerable assumptions about the averaged temperature profile and of the nature of the radiative heating. Another feature of the system which is currently missing from our model, is a more careful analysis of the fact that the whole cylinder assembly is constantly moving (in an axial direction) through the laser beam. This will need to be studied in further investigations.

Report written by Chris Budd, Bath. April 2009.

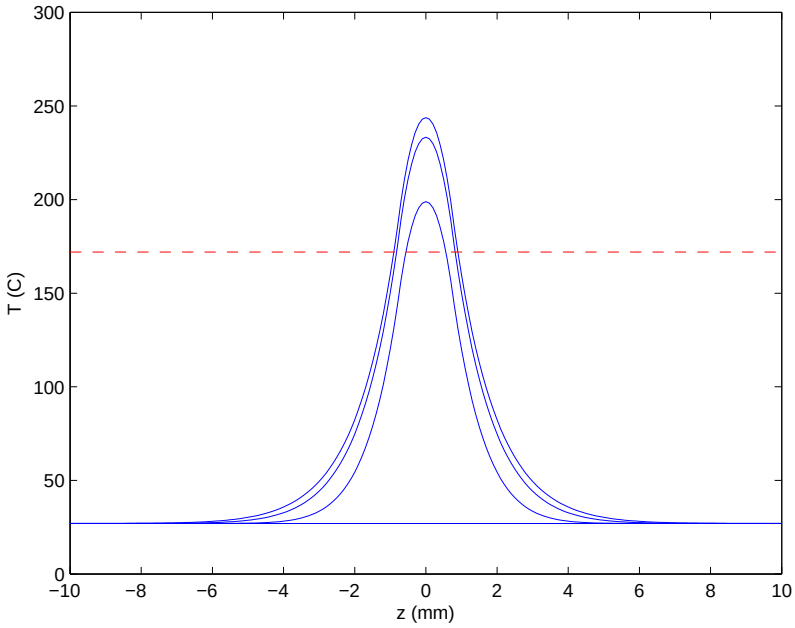

Figure 5: The averaged temperature $\bar{T}(z,t)$ as a function of z for various times $t = 0s, 10s, 20s, 30s$. The melting point of the Pebax is indicated by the dotted line

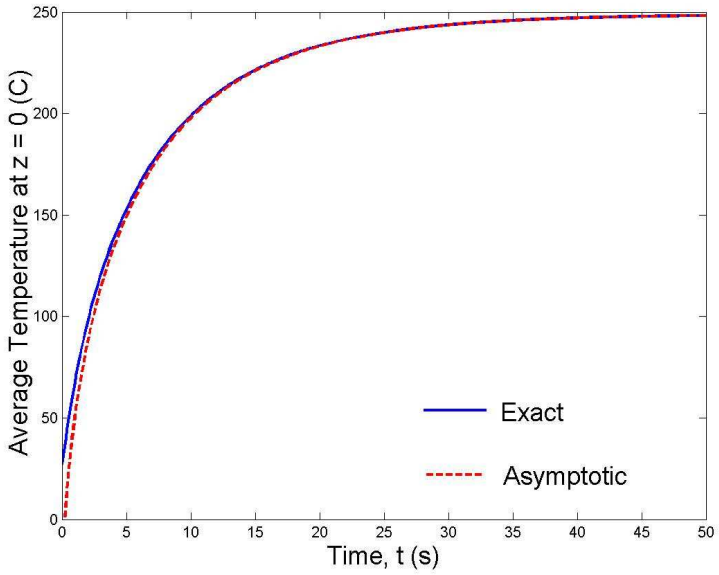

Figure 6: The centre temperature $\bar{T}(0,t)$, comparing the exact and the asymptotic solutions.